



# The Impact of Diaphragm Stiffness on the Wind-induced Lateral Force Resistance of Concrete Modular Buildings

Jing Li\*<sup>ORCID</sup> and Yuyang Jiang<sup>ORCID</sup>

School of Civil Engineering and Transportation, South China University of Technology,  
Guangzhou 510641, China  
cvjingli@scut.edu.cn

**Abstract.** The diaphragm's continuous integrity is vital to the lateral resistance capacity of buildings. However, there is a paucity of research concerning the impact of diaphragm stiffness in concrete modular structures, impeding their broader adoption in high-rise construction. This study employs ETABS to investigate the role of diaphragm stiffness on wind-induced lateral force resistance in concrete modular buildings without a core tube (NCS). Findings reveal that in NCS configurations, the in-plane axial and out-of-plane normal stiffnesses of horizontal connections exert a more substantial influence on the structure's lateral force resistance compared to the in-plane shear stiffness. Notably, any decrease in normal stiffness can result in pronounced structural displacements that are non-negligible. Analysis of the periods and lateral displacements suggests that a diaphragm stiffness coefficient not exceeding 0.5 is imperative for ensuring optimal lateral force resistance. All structures examined herein, featuring diverse diaphragm stiffness configurations, comply with the specified lateral displacement limits.

**Keywords:** concrete modular building, diaphragm stiffness, horizontal connection, lateral force resistance.

## 1 Introduction

In recent years, China has vigorously promoted green construction methods. Modular construction, which uses prefabricated three-dimensional modules made in factories and assembled on-site to form permanent buildings, can solve the manual labor problem in the construction industry [1-6].

The characteristic of using rule repeating modules in modular architecture reveals that it is more suitable for high-rise buildings in metropolitan areas with limited available land resources [7]. Unlike mid to low rise buildings, high-rise building structures are often more controlled by horizontal loads such as wind loads [8]. These horizontal loads are transmitted through the diaphragm to the vertical components that resist lateral forces, and finally to the foundation. The first part of the transmission path consists the diaphragm system. The dramatically lateral displacement or even collapse can occur if the diaphragm performance cannot be satisfied.

As the inter-module connections become the weakest part of the structure subjected to horizontal forces such as earthquakes and wind loads. Researches on modular buildings mainly includes the study of connection nodes and the lateral force resistant systems. The modular building includes steel structures and concrete structures. There are more researches on modular building nodes and lateral force resistant systems of steel structures. Therefore, steel modular structure applications are more mature. Chen [9] proposed a reference formula for the tensile and shear bearing capacity of rotating connections of modular steel structures through experiments. Yu [10] and Chua [11] respectively studied the vertical components and load transfer of steel modular buildings lateral resisting system by simplified models, and verified the accuracy of the proposed simplified models. Srisangeerthan [12] studied the effect of diaphragm stiffness changes under seismic loads on the lateral resisting system performance of steel modular buildings by simplified model, indicating that an increase of diaphragm flexibility leads to higher modal participation in the structures.

In contrast to steel modular buildings, conventional concrete modular buildings typically use cast-in-place concrete for inter-module connections, which is both time-intensive and laborious. Pan [13] introduced a simplified spring model that considers in-plane axial and shear characteristics to simulate horizontal connections in a finite element analysis. This study systematically investigates the impact of horizontal connections on the wind-induced structural response of a case building, indicating the feasibility of the discrete diaphragm system.

The studies on non-modular building systems can provide reference. Zhao [14] studied the influence of diaphragm deformation on the structural system using a 12-story frame shear wall structure model. The results showed that considering the influence of diaphragm deformation can better reflect the actual working situation of the structures.

This paper employs ETABS to investigate the impact of diaphragm stiffness on the wind-induced lateral force resistance performance of concrete modular buildings. Analysis focuses on the configuration without a central core tube (NCS), featuring horizontal interconnections between modules. These interconnections are characterized by their in-plane axial stiffness, out-of-plane normal stiffness, and in-plane shear resistance. Initially, the research separately examines the lateral displacement of NCS structure under varying stiffness combinations subjected to wind loads. This analysis elucidates the distinct roles of connection stiffnesses in controlling the lateral displacement behavior. Subsequently, to deepen understanding of diaphragm stiffness effects, the study further explores how modifications to diaphragm stiffness influence parameters such as lateral displacement and natural periods, thereby augmenting existing research in this domain.

## 2 Structural model

### 2.1 Structural Selection and Layout

A 20 story NCS is shown in Figure 1. The NCS consists of 180 concrete modules, with a size of  $4.5\text{m} \times 3\text{m}$  (length  $\times$  width) and a story height of 3m. The module wall thickness is 150mm and the diaphragm thickness is 200mm. The structure is entirely made of C40 concrete.

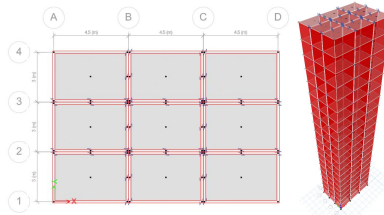


Fig.1. Structural layout plan and 3D diagram

### 2.2 Connection Types

In order to focus on the influence of horizontal connections on the lateral force resistance performance of concrete modular structures under wind loads, the following simplifications were made to the model:

(1) Vertical module walls are connected using cast-in-place connections, while horizontal modules are connected using simplified spring connections that consider in-plane axial stiffness, in-plane shear stiffness, and out-of-plane normal stiffness.

(2) Assuming there is no misalignment between the upper and lower modules.

The schematic diagram of horizontal connection deformation between diaphragms is shown in Figure 2. When X-direction wind load is applied, the connection mainly produces in-plane axial deformation and out-of-plane normal shear deformation. When the Y-direction wind load is applied, the connection mainly produces in-plane shear deformation, and out-of-plane normal deformation.

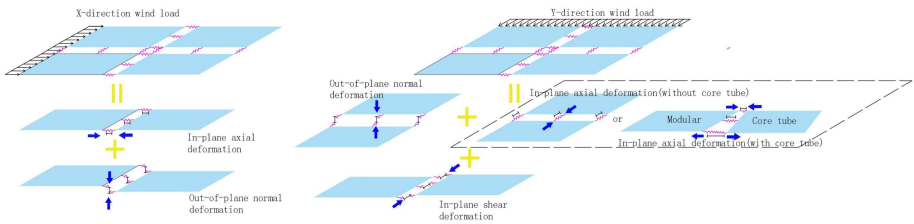


Fig.2. Schematic diagram of horizontal connection deformation

The diaphragm of each module or adjacent corridor slab is a continuous and rigid overall diaphragm, and the diaphragms are connected by the above horizontal connections (as shown in Figure 3). In the NCS, horizontal connections are arranged in a bidirectional manner. The diaphragms between every two adjacent modules are connected through three horizontal connections.

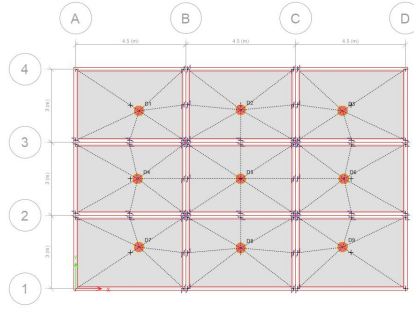


Fig. 3. Schematic diagram of flexible diaphragm system layout

### 3 Comparison of lateral displacements of models with different stiffness connections

Six models: IS12, IS13, IS23, IS123 and two cast-in-place models (R and SR) are studied in the analysis. The models IS<sub>12</sub>, IS<sub>13</sub>, IS<sub>23</sub>, and IS<sub>123</sub> incorporate varying connection stiffness combination - namely in-plane axial, out-of-plane normal, and in-plane shear - where subscripts 1, 2, and 3 denote the in-plane axial stiffness, out-of-plane normal stiffness, and in-plane shear stiffness of the horizontal connection of  $10^{12}$  kN/m and the untreated stiffness of 0 respectively. The R model represents a conventionally cast-in-place diaphragm and the SR model signifies a semi-rigid diaphragm, accounting for actual stiffness and the influence of diaphragm elasticity on the building. Calculate the maximum diaphragm displacement curves under the X-direction and Y-direction wind load respectively via ETABS. Application of wind loads in ETABS is segmented into diaphragm and shell objects. In this work, uniform X-direction and Y-direction wind loads are applied to the shell object. Calculate the maximum diaphragm displacement curves of the IS models and cast-in-place model of the modular structures without core tube under the action of X-direction wind load and Y-direction wind load, as shown in Figure 4.

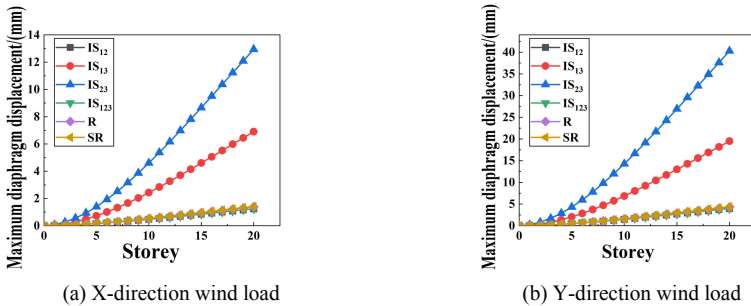


Fig. 4. Maximum diaphragm displacement curves

From the curve, it can be seen that the structural lateral displacement is  $IS_{23} > IS_{13} > IS_{12}$ , and the lateral displacement controlled by stiffness in three directions is in-plane axial > out-of-plane normal > in-plane shear. From this, it can be concluded that in NCS, a decrease in the normal stiffness of horizontal connections will lead to significant lateral displacement that cannot be ignored. In addition, the change in shear stiffness of horizontal connections has a very small impact on the lateral displacement of the structural system.

It is worth noting that the in-plane shear stiffness has a very small impact on the lateral displacement of the NCS. This conclusion is not because this structural system has horizontal connections arranged vertically and horizontally, which weakens the effect of shear stiffness in the connection plane, but because the displacement of the connections between modules is not obvious along the local 3-axis. As shown in Figure 5, when the NCS is disconnected along the Y direction and the axial and normal stiffness of the connection is  $10^{12} \text{ kN/m}$ , the shear stiffness in the structural plane changes from 0 to  $10^{12} \text{ kN/m}$ , and the lateral displacement of the structure still does not change significantly (Figure 6). The reason for using longitudinal and transverse arrangement nodes is to amplify the displacement changes in the Y-direction under the action of Y-direction wind load, so as to facilitate the subsequent connection stiffness values representing different diaphragm stiffness.

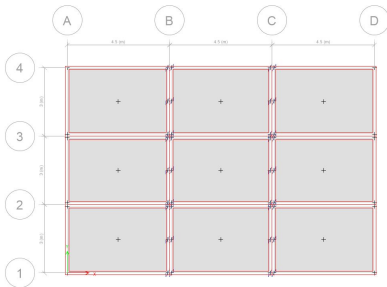


Fig. 5. Plan layout without Y-direction connection

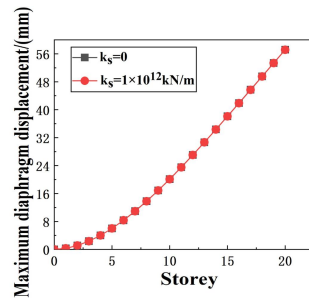


Fig. 6. Comparison of Y-axis lateral displacement without Y-axis connection

## 4 Method for determining the stiffness of connections

### 4.1 Coefficient of change in diaphragm stiffness $\alpha$

For the NCS, the stiffness of the diaphragm is changed by changing the stiffness value of the stiffness combination considered for horizontal connections, and the influence of diaphragm stiffness on the lateral force resistance performance of the NCS is studied. To measure the rigidity of the diaphragm, the stiffness coefficient of the diaphragm is introduced  $\alpha$ :

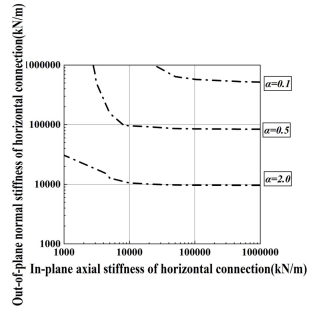
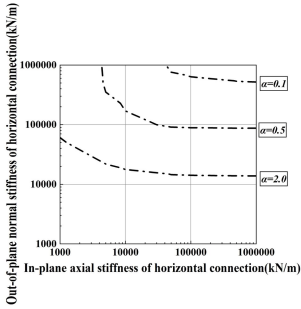
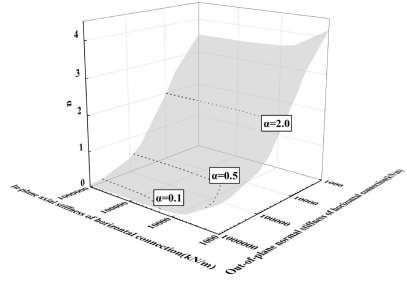
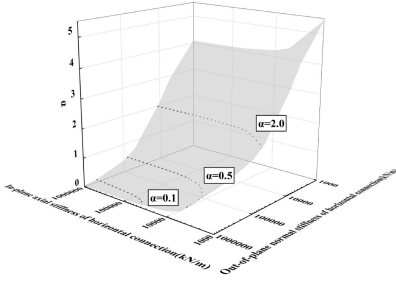
$$\alpha = \frac{\Delta_F - \Delta_R}{\Delta_R} = \frac{\Delta_I}{\Delta_R} \tag{1}$$

Among them:  $\Delta_F$  is the displacement of the top layer of the structure with a relatively flexible diaphragm system;  $\Delta_R$  is the displacement of the top layer of the IS system structure;  $\Delta_i$  is the increase in displacement of the top layer of the structure due to the relative flexibility of the diaphragm.

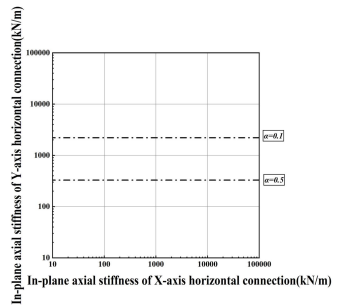
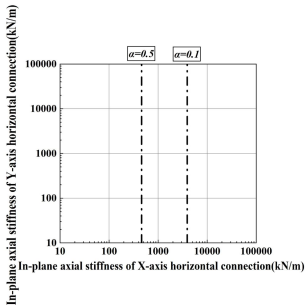
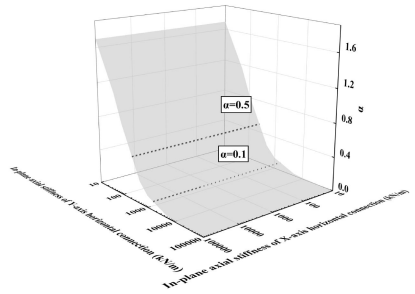
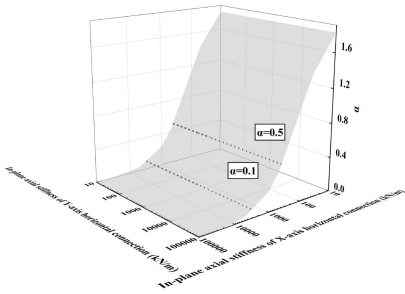
According to some regulations and literature standards [15-17], when  $\alpha < 0.5$ , the diaphragm is defined as rigid; When  $0.5 < \alpha < 2.0$ , the diaphragm is defined as semi rigid; When  $\alpha > 2.0$ , the diaphragm is defined as flexible. This standard is mostly used to measure mid to low rise buildings, but being too conservative for high-rise buildings may lead to structural failure. Therefore, a stricter definition should be made [13]: when  $\alpha < 0.1$ , define the diaphragm as rigid; When  $0.1 < \alpha < 0.5$ , the diaphragm is defined as semi rigid; When  $\alpha > 0.5$ , the diaphragm is defined as flexible.

#### 4.2 Horizontal Connection Stiffness Values

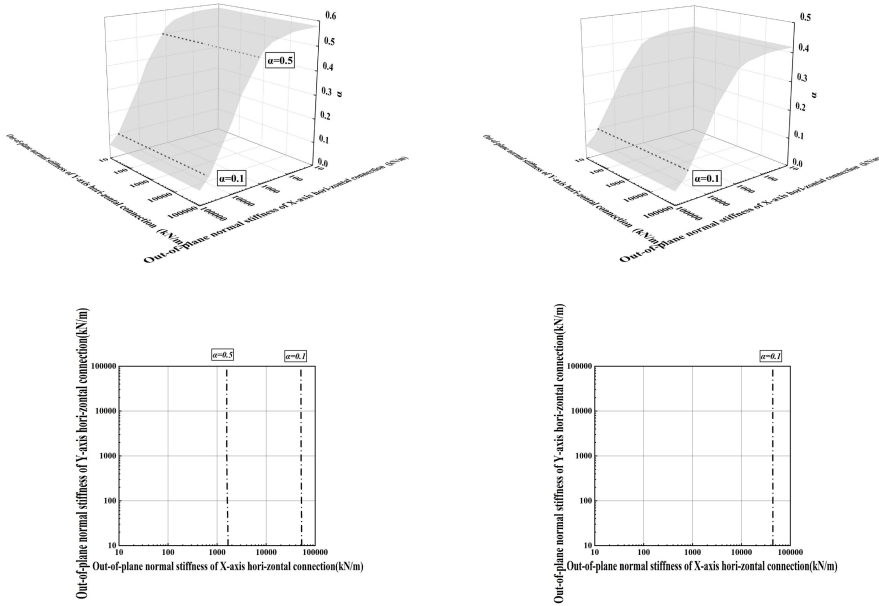
Three combinations participate in the analysis. Considering that the combination of in-plane axial stiffness and out-of-plane normal stiffness is ZH-12, the combination of in-plane axial stiffness and in-plane shear stiffness is ZH-13, and the combination of out-of-plane normal stiffness and in-plane shear stiffness is ZH-23. By changing the stiffness values of different combinations of horizontal connections (with a range of 10kN/m~10<sup>6</sup>kN/m for X-axis and Y-axis stiffness), the lateral displacement of the NCS in the X and Y directions was calculated. Then, the contour maps of target  $\alpha$  were calculated and organized for different connection stiffness, and the contour map of target  $\alpha$  was obtained (as shown in Figure 7). The values of different horizontal connection stiffness are shown in Table 1. From the previous text, it can be concluded that the in-plane shear stiffness of horizontal connections in NCS has little effect on the lateral displacement of the structure. Therefore, when considering ZH-13 and ZH-23, the actual control values for the  $\alpha$  values in the X and Y directions of the structure are the in-plane axial stiffness and the out-of-plane normal stiffness of the horizontal connection respectively. Moreover, there are unique axial stiffness and normal stiffness values corresponding to the  $\alpha$  values in the X and Y directions of the structure, as shown in Figures 7b and 7c. The above unique values can be directly taken for the horizontal connection stiffness values. When considering ZH-12 (as shown in Figure 7a), the maximum deflection point of the  $\alpha$  value contour lines in the X and Y directions of the structure can be taken separately. The connection stiffness can be adjusted according to the  $\alpha$  value of the structure in the input software to determine the connection stiffness representing different  $\alpha$  values.



(a) ZH-12 under X-direction wind load (left) and Y-direction wind load (right)



(b) ZH-13 under X-direction wind load (left) and Y-direction wind load (right)



(c) ZH-23 under X-direction wind load (left) and Y-direction wind load (right)

Fig.7  $\alpha$  3D surface and contour map

Table 1. Horizontal connection stiffness values for different stiffness combinations (kN/m)

Structural $\alpha$ value		$\alpha=0.1$	$\alpha=0.5$	$\alpha=2.0$
ZH-12	In-plane axial stiffness of horizontal connection	90000	10000	5000
	Out-of-plane normal stiffness of horizontal connection	550000	92000	12000
ZH-13	In-plane axial stiffness of X-axis horizontal connection	3900	460	/
	In-plane axial stiffness of Y-axis horizontal connection	2200	330	/
ZH-23	Out-of-plane normal stiffness of X-axis horizontal connection	51000	1600	/
	Out-of-plane normal stiffness of Y-axis horizontal connection	35000	10	/

## 5 Parameter impact analysis

Input different connection stiffness representing different  $\alpha$  values into the model, further analyze the comprehensive impact of different horizontal connection stiffness on the structural response of NCS under wind load.

### 5.1 Structural inherent period analysis

As shown in Figure 8, in the NCS, the periods of each vibration mode of the structure decrease with the increase of diaphragm stiffness. When the out-of-plane normal stiffness is not considered, the flexible diaphragm system can maintain a basically unchanged natural vibration period of the structure along the two horizontal axes;

When considering the out-of-plane normal stiffness, the period of each vibration mode of the structure increases as the stiffness of the diaphragm decreases. In addition, when considering ZH-12, the periods of the cast-in-place structure are significantly greater than that of  $\alpha=0.1$  and  $\alpha=0.5$ , as well as the IS<sub>12</sub> structural system. This is mainly due to the limited stiffness of the cast-in-place structure diaphragm in the out-of-plane normal direction, which cannot reach the stiffness values set in the software connections.

Regarding the first four vibration modes of the structure, When considering ZH-12, only when  $\alpha=0.1$  matches well with the first four vibration modes of the IS<sub>12</sub> structure, while when  $\alpha=0.5$  and  $\alpha=2.0$ , only the first vibration mode (translational along the Y-direction of the structure) matches well with the IS<sub>12</sub> structure; When considering ZH-13, the first three vibration modes of  $\alpha=0.1$  and  $\alpha=0.5$  are in good agreement with the IS<sub>13</sub> structure; When considering ZH-23, both the IS<sub>13</sub> model and different  $\alpha$  models exhibit abnormal vibration modes, and the first and second vibration modes are not conventional (translational along the X-axis or Y-axis of the structure). It can be seen that in order to ensure that the NCS has similar structural response to the IS model, the  $\alpha$  value should not exceed 0.5. In addition, due to the significant impact of in-plane axial stiffness changes on the X-direction displacement of the structures, considering ZH-23 is not an ideal choice.

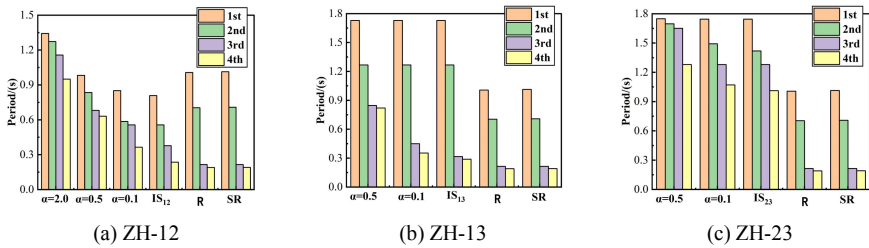


**Fig. 8.** Comparison of structural periods with different diaphragm stiffness under different stiffness combinations

### 5.2 Structural lateral displacement analysis

As shown in Figure 9, due to the fact that the lateral resisting system of NCS is only composed of shear walls, the lateral displacement of NCS shows a bending shape. The lateral displacement of NCS increases with the decrease of the diaphragm stiffness. According to the specification [18], the limit value of story drift for reinforced concrete shear wall structures is 1/1000. Only when considering ZH-23 under Y-direction wind load, the structural  $\alpha=0.5$  does not meet the requirements.

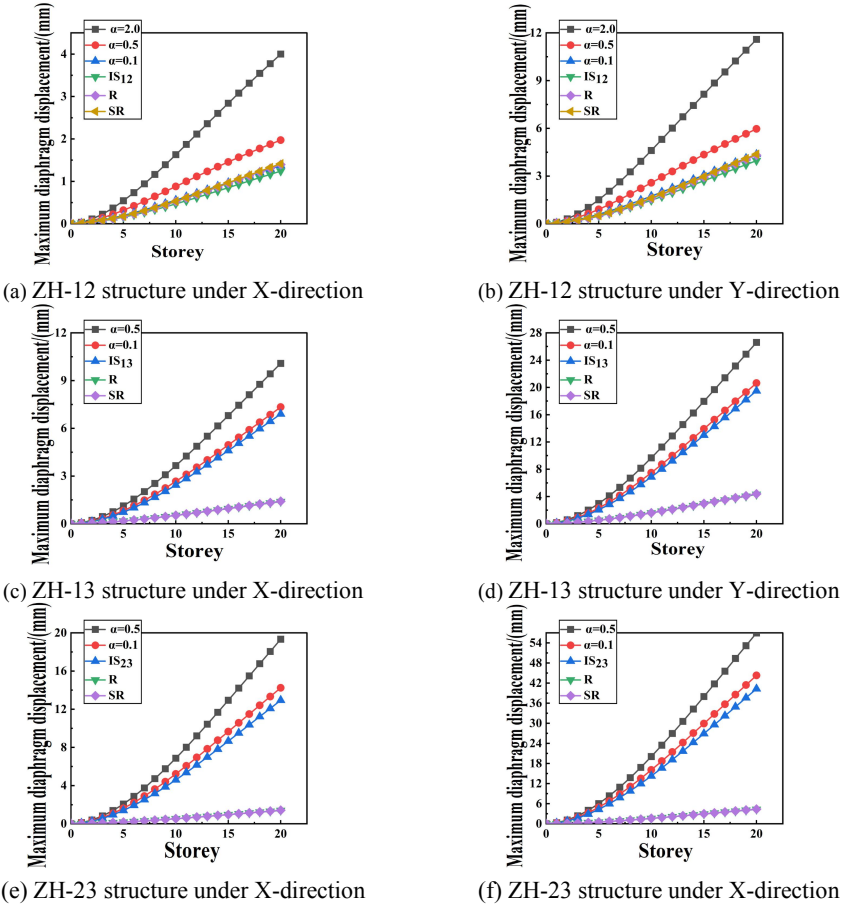


Fig. 9. Comparison of lateral displacement of structures with different diaphragm stiffness under wind load under different stiffness combinations

## 6 Conclusion

1) In the NCS, the in-plane axial stiffness and out-of-plane normal stiffness of connections have a much greater impact on the lateral force resistance performance of the structure than the in-plane shear stiffness. Especially, the reduction of normal stiffness can lead to significant displacement of the structural system that cannot be ignored;

2) In the NCS, the vibration mode periods of the structure decrease with the increase of diaphragm stiffness. In order to ensure better lateral force resistance performance, the value of the diaphragm stiffness coefficient of the structure should not exceed 0.5.

3) In the NCS, the lateral displacement of each discrete diaphragm system structure decreases with the increase of diaphragm stiffness. The structures considered in this

article with different combinations of diaphragm stiffness meet the lateral displacements requirements of the specifications.

## References

1. Pan, W, Hon C K.: Modular integrated construction for high-rise buildings. *Proceedings of the Institution of Civil Engineers* 173(2), 64-68 (2018).
2. Yang Y, et al.: Sources of Uncertainties in Offsite Logistics of Modular Construction for High-Rise Building Projects. *Journal of Management in Engineering* 37(3), 4021011 (2021).
3. Liu Q, et al.: The current development status and future prospects of modular assembly buildings. *Journal of Qingdao University of Technology* 42 (05), 35-40+48 (2021).(in Chinese)
4. Fan H, Han J Z.: Application Analysis of Modular Architecture in Emergency Construction. *Housing Industry (Z1)*, 32-40 (2020). (in Chinese)
5. Srisangeerthanan S, et al.: Review of performance requirements for inter-module connections in multi-story modular buildings. *Journal of Building Engineering* 28, 101087 (2020).
6. Zheng Z, Zhang Z, Pan W.: Virtual prototyping and transfer learning-enabled module detection for modular integrated construction. *Automation in Construction* 120, 103387 (2020).
7. Liew J Y R, Chua Y S, Dai Z.: Steel concrete composite systems for modular construction of high-rise buildings. *Structures* 21, 135-149 (2019).
8. Su R K L, Tang T O, Liu K C.: Simplified seismic assessment of buildings using non-uniform Timoshenko beam model in low-to-moderate seismicity regions. *Engineering Structures* 120, 116-132 (2016).
9. Chen Z, et al.: Tensile and shear performance of rotary inter-module connection for modular steel buildings. *Journal of Constructional Steel Research* 175, 106367 (2020).
10. Yu Y, Z Chen.: Rigidity of corrugated plate sidewalls and its effect on the modular structural design. *Engineering Structures* 175, 191-200 (2018).
11. Chua Y S, Liew J Y R, Pang S D.: Modelling of connections and lateral behavior of high-rise modular steel buildings. *Journal of Constructional Steel Research* 166, 105901 (2020).
12. Srisangeerthanan S, et al.: Numerical study on the effects of diaphragm stiffness and strength on the seismic response of multi-story modular buildings. *Engineering Structures* 163, 25-37 (2018).
13. Pan W, Wang Z, Zhang Y.: Novel discrete diaphragm system of concrete high-rise modular buildings. *Journal of Building Engineering* 51, 104342 (2022).
14. Zhao X A.: Calculation of high-rise building structure considering diaphragm deformation. *China Civil Engineering Journal* (04),25-30 (1983).
15. ASCE/SEI 7-10, Minimum Design Loads for Buildings and Other Structures, American Society of Civil Engineers, Reston, 2010.
16. NZS 1170.5, Structural Design Actions: Part 5: Earthquake Actions-New Zealand, Standards New Zealand, Wellington, 2004.
17. AS 1170.4, Structural Design Actions: Part 4: Earthquake Actions in Australia, Standards Australia, Sydney, 2007.
18. JGJ3-2010 (Technical specifications for concrete structures of high-rise buildings). China Construction Industry Press, Beijing (2010). (in Chinese)

**Open Access** This chapter is licensed under the terms of the Creative Commons Attribution-NonCommercial 4.0 International License (<http://creativecommons.org/licenses/by-nc/4.0/>), which permits any noncommercial use, sharing, adaptation, distribution and reproduction in any medium or format, as long as you give appropriate credit to the original author(s) and the source, provide a link to the Creative Commons license and indicate if changes were made.

The images or other third party material in this chapter are included in the chapter's Creative Commons license, unless indicated otherwise in a credit line to the material. If material is not included in the chapter's Creative Commons license and your intended use is not permitted by statutory regulation or exceeds the permitted use, you will need to obtain permission directly from the copyright holder.

